



ELŻBIETA HYCNR\*

## The structural and textural characteristics of limestones and the effectiveness of SO<sub>2</sub> sorption in fluidized bed conditions

### Introduction

A number of technologies to reduce SO<sub>2</sub> emissions from the power industry have been developed. However, only some of them have been applied in practice. Calcium methods are the most commonly used both in Poland and Europe. They are used in 99% of the existing flue gas desulphurization installations in the Polish power industry (Galos et al. 2016). They are based on the binding of sulphur dioxide from flu gases using calcium sorbents, which include: limestones (CaCO<sub>3</sub>), burnt lime (CaO), and hydrated lime (Ca(OH)<sub>2</sub>). In Poland, the process of binding of sulphur dioxide uses mostly limestone that is ground to the desired granulation. Based on the method of feeding the sorbent to the combustion chamber and the character of the desulphurization product, the mentioned methods are classified as dry (both in pulverized and fluidized bed boilers), semi-dry, and wet. Wet methods are the most commonly used in large power plants. Although the mentioned methods require substantial capital investment, they guarantee a high efficiency of flue gas desulphurization (<95%) and a stable product of desulphurization process in the form of gypsum. Semi-dry methods require less capital investment, but are characterized by lower flue gas desulphurization efficiency compared to wet methods (60–80%). In addition, the obtained desulphurization product – calcium sulphate IV (CaSO<sub>3</sub>) is a highly unstable waste. The most problematic,

---

\* Ph.D. Eng., AGH University of Science and Technology, Krakow, Poland; e-mail: ehycnar@wp.pl

because of the lowest desulphurization efficiency (35–50% pulverized fuel boilers), are dry methods. Their undoubted advantage is that they require the lowest investment and operating expenditures and provide a stable desulphurization product in the form of calcium sulphate anhydrite. At the same time, they are suitable for use in fluidized bed technology, including all types of boilers. The sorbent, in the form of ground limestone (with a grain size in the range 0.1–1.2 mm) is fed directly into the boiler without the need for an additional desulphurization installation. The low efficiency of SO<sub>2</sub> capture remains a problem. To solve this problem, the sorbent is added to the boiler in excess amounts relative to the SO<sub>2</sub> content in the flue gas. This leads to an increase in the amount of furnace waste and the unreacted CaO, which is accompanied by the unsatisfactory efficiency of the desulfurization process. It Upgrading the existing fluidized bed combustion boilers with wet flue gas desulphurization installations was also suggested. This results in low SO<sub>2</sub> emissions but significantly increases the cost of energy production.

The desulphurization during the combustion in fluidized bed boilers is the second, after the wet lime method, most popular technological solution. The studies on the efficiency of the desulphurization of lime sorbents under fluidized bed conditions have been conducted for more than 40 years. It has been shown that the effectiveness of SO<sub>2</sub> sorption depends on many factors, including the furnace construction, boiler feeding method, the fuel combustion temperature, the sorbent grain diameter, and the sorbent residence time in the furnace (Borgwardt 1985; Mohmmand et al. 1988; Szymanek and Nowak 2007). It was not possible to clearly indicate which sorbent parameters are responsible for the efficiency of desulphurization in fluidized bed boilers. There were attempts to link the SO<sub>2</sub> sorption efficiency with the geological age of limestones, which would be proven by the fact that the younger limestones (e.g. Jurassic) are more reactive than the older ones (e.g. Permian or Devonian) (Dam-Johansen and Østergaard 1991; Antony and Granatstein 2001). However, this is not entirely true, because limestones from the same deposit often have a different efficiency of SO<sub>2</sub> capture, even though their CaCO<sub>3</sub> content is similar (Antony and Granatstein 2001; Szymanek and Nowak 2007). Therefore, the reactivity of limestone should not be directly related to the geological age and the processes of diagenesis and epigenesis, mainly related to the dissolution and recrystallisation of calcite (Yrjas et al. 1995). Older rocks are generally characterized by much stronger diagenesis, which is manifested by a solid rock texture and a more crystalline structure, made up of larger calcite crystals. Younger rocks are usually characterized by a weaker diagenesis, a porous texture, and microcrystalline structure. These dependencies should not, however, be directly related to the geological age of the rock and hence the geological age of the limestone should not be a determinant of their reactivity.

The studies on the reactivity of limestone in relation to the SO<sub>2</sub> presented in this paper have been conducted for several years. They were inspired by the problems of Polish power plants and CHP plants in meeting the SO<sub>2</sub> emission limits when using limestones as SO<sub>2</sub> sorbents in fluidized bed boilers and related to their low utilization and storage, and the high content of unreacted CaO in the ash. Several hundred samples of these rocks were ex-

amined as part of the research aimed at demonstrating the sorption properties of limestone used in the Polish power industry. The samples were collected from the currently exploited Polish limestone deposits and other deposits, in which limestone is an accompanying mineral. Cretaceous (chalk), Jurassic, Triassic, Devonian, and Neogene (lacustrine chalk) limestones were analyzed. The results of the study confirmed the conclusions of other researchers that the reactivity of calcium does not depend on the  $\text{CaCO}_3$  content. The samples of Jurassic limestone, collected from the overburden of the Zalas porphyry deposit, with the  $\text{CaCO}_3$  content in the range 95–99% by weight and the reactivity at the level of 2.32–2.58 mol Ca/mol S (Hycnar et al. 2012), and the samples of lacustrine chalk, where, in some cases, the content of calcium carbonate was only 68% by weight and the reactivity was relatively high – 1.63 mol Ca/mol S (Hycnar et al. 2016) were examined. It has been suggested that the reactivity is not related to the size of the surface area. Despite their small specific surface area ( $S_{\text{BET}} = 1.19 \text{ g/m}^2$ ), the Upper Jurassic limestones from the Bełchatów lignite deposit are characterized by a high reactivity  $\text{RI} = 1.85 \text{ mol Ca/mol S}$  (Hycnar et al. 2015). In turn, the above-mentioned limestones from the Zalas porphyry deposit, despite the well-developed surface area ( $S_{\text{BET}} = 4.13 \text{ g/m}^2$ ), are characterized by a significantly weaker reactivity ( $\text{RI} = 2.32 \text{ mol Ca/mol S}$ ) (Hycnar et al. 2012). It has been observed, however, that the  $\text{SO}_2$  sorption efficiency increases with the degree of development of the sorbent's specific surface during the thermal dissociation, provided that the porosity of mesopores and macropores is being increased. The results of the research are shown on the example of Jurassic limestones from the previously mentioned Bełchatów lignite deposit. The Bełchatów deposit is the largest currently exploited lignite mine in Poland. It belongs to tectonic-type deposits. The coal occurs within the Kleszczów tectonic graben, formed in Jurassic and Cretaceous sediments including limestone and marl. The Kleszczów graben sets the boundaries (slopes) of the mining excavation (Fig. 1). In order to ensure the stability of slopes during



Fig. 1. Bełchatów lignite mine, the Szczerców exploitation field. Exposure of the limestone floor at the IVth exploitation level, in the ordinate range of +112/+81 m above sea level

Rys. 1. Złoże węgla brunatnego Bełchatów, Pole eksploatacyjne Szczerców.  
Odslonięcie stropu wapieni na IV poziomie eksploatacyjnym, w zakresie rzędnych +112/+81 m n.p.m.

the extraction of coal, it is necessary to form them to the desired dip angle. For this reason, the limestones within the slopes can be successively exploited. The research material was 185 limestone samples collected from 33 boreholes.

## 1. The research methodology and the procedure of the analysis

In the first stage of the study, the limestone samples were subjected to the sulphation process carried out according to the guidelines developed by the Ahlstrom Pyropower Development Laboratory (Alsthrom... 1995). This method is based on determining two indicators: the reactivity (RI) and absolute sorption (CI – capacity index). The reactivity index determines the ratio of the calcium content in the sample to the amount of sulphur after the sorption process [Ca/S moles]. The absolute sorption index CI, in turn, determines the amount of sulphur sorbed by 1000 g of the sorbent [g S/1000 g of the sorbent]. The SO<sub>2</sub> sorption studies were carried out using a material with a particle size of 0.125–0.250 mm. As required, the samples were subjected to a decarbonization process at 850°C for 30 minutes prior to the sulphation. Then, a gas containing 1780 ppm of SO<sub>2</sub>, 3% of O<sub>2</sub>, and 16% of CO<sub>2</sub> was passed through the samples with a speed of 950 ml/second for another 30 minutes. In the next stage, the content of the sorbed sulfur was determined using a LECO analyzer. Based on the results obtained, the RI and CI indexes were determined and the sorption capacity was assessed based on the reference values of the mentioned parameters (Table 1).

In the next stage of the study, an attempt to define the sorbent parameters affecting its reactivity was made. The analysis was aimed at:

- ◆ Determining the mineral composition, petrographic nature, and structural and textural characteristics of the examined limestones. For this purpose, X-ray diffraction, optical and scanning microscopy were applied.

Table 1. The reference values of the reactivity (RI) [Ca moles/S moles] and the absolute sorption (CI) [g S/ 1000 g of the sorbent] (Alsthrom Propywer 1995)

Tabela 1. Wartości wzorcowe wskaźnika reaktywności (RI) [Ca mol/S mol] i sorpcji bezwzględnej [g S/ 1000 g sorbentu] (Alsthrom Propywer 1995)

The sorption capacity of the sorbent	RI	CI
Excellent	< 2.5	> 120
Very good	2.5–3.0	100–120
Good	3.0–4.0	80–100
Sufficient	4.0–5.0	60–80
Low quality	> 5.0	<60

- ◆ Determining the chemical composition of the examined limestones. Determining the content of  $\text{CaCO}_3$ ,  $\text{SiO}_2$ ,  $\text{Al}_2\text{O}_3$ ,  $\text{MgO}$ ,  $\text{K}_2\text{O}$ ,  $\text{Na}_2\text{O}$ ,  $\text{Fe}_2\text{O}_3$ ,  $\text{Mn}_2\text{O}_3$ , and  $\text{TiO}_2$ . The analysis was performed using Atomic Absorption Spectrometry (AAS) and Atomic Emission Spectrometry (ICP-AES).
- ◆ Determining the temperature and the degree of calcite decomposition on the basis of derivatographic investigation (DTA, TG, and DTG).
- ◆ Determining the parameters of the porous texture of limestones on the basis of the low temperature nitrogen adsorption method by calculating the specific surface area ( $S_{\text{BET}}$ ) according to the Brunauer – Emmet – Teller method, the total pore volume ( $V_{\text{tot}}$ ) for the relative pressure  $p/p_0 = 0.99$ , the micropore volume ( $V_{\text{mic}}$ ) (pores with a diameter less than 2 nm) and their share in the total pore volume ( $V_{\text{mic}}/V_{\text{tot}}$ ) according to the Dubinin – Radushkevich equation, the mesopore volume ( $V_{\text{mes}}$ ) (pores with a diameter greater than 2 nm and less than 50 nm) and their share in the total pore volume ( $V_{\text{mes}}/V_{\text{tot}}$ ) according to the Barrett – Joyner – Halenda (BJH) approach, and the macropore volume ( $V_{\text{mac}}$ ) (pores with a diameter larger than 50 nm) by subtracting the micro- and mesopore volume ( $V_{\text{mac}} = V_{\text{tot}} - (V_{\text{mic}} + V_{\text{mes}})$ ) and their share in the total pore volume ( $V_{\text{mac}}/V_{\text{tot}}$ ) from the total pore volume.
- ◆ A porous texture analysis was performed using mercury porosimetry. The following porous texture parameters were determined:
  - ◆ The coefficient of effective porosity, that is the ratio of pore volume to the external volume of the sample (Such 2000, 2002; AutoPore... 2008):

$$\phi = \frac{V_{\text{tot}}}{V_b} \cdot 100\% = \frac{V_b - V_s}{V_b} \cdot 100\% = \left(1 - \frac{\rho_b}{\rho_s}\right) \cdot 100\%$$

- ↗  $\phi$  – The coefficient of effective porosity [%],
- $V_b$  – External volume [ml],
- $V_s$  – Skeletal volume [ml].

- ◆ The specific surface area of porous space, that is the total pore area in relation to the unit weight of material. This parameter characterizes the flow resistance of reservoir media in the porous medium. The specific surface area, assuming the reversibility of the injection process is determined on the basis of the obtained pore volume according to the following equation (Rootare and Prenzlow 1967; Such 2000):

$$A = -\frac{1}{\gamma \cos \theta} \int_0^V P dV$$

- ↗  $A$  – The total surface area of porous space [ $\text{m}^2 \cdot \text{g}^{-1}$ ],
- $dV$  – Partial pore volume corresponding to the capillary pressure required [ $\text{m}^3$ ],

- $P$  – Capillary pressure [psi],  
 $\gamma$  – Surface tension of mercury [ $\text{dyne}\cdot\text{cm}^{-1}$ ],  
 $\theta$  – Contact angle [ $^{\circ}$ ].

- The average pore diameter ( $D_{av}$ ) is weighted with the weight of the pore size for the entire pore diameter range in the sample (Such 2000) and is calculated using the following equation (AutoPore... 2008):

$$D_{sr} = \frac{4 \cdot V_{tot}}{A}$$

↪  $D_{av}$  – the average pore diameter [ $\mu$ ].

In order to characterize the decarbonization and  $\text{SO}_2$  sorption processes, the mentioned texture parameters were determined for both the decarbonized and sulphated samples.

## 2. Results

The reactivity (RI) and total sorption (CI) indices for the examined limestones, determined in accordance with the guidelines developed by the Ahlstrom Pyropower Development Laboratory (Ahlstrom 1995) are highly variable. The RI index is in the range from 1.97 to 3.1 Ca/S moles and the CI index is between 160.85 and 99.85 gS/1000 g of the sorbent. The sorption properties of the examined limestones range from excellent to good.

The chemical composition of the examined limestones (Table 2) is significantly less variable. The most important parameter, the  $\text{CaCO}_3$  content is in the range 91.11–99.15% by weight.

In order to determine the limestone parameters affecting its reactivity, the samples with the highest  $\text{CaCO}_3$  content (Table 3) and with significantly different RI and CI values were selected for further analysis (Table 4).

Table 2. The chemical composition of limestone samples from the Belchatów deposit, the Szczerców exploitation field (% by weight)

Tabela 2. Skład chemiczny próbek wapieni ze złoża Belchatów, Pole eksploatacyjne Szczerców (% wag.)

	$\text{SiO}_2$	$\text{TiO}_2$	$\text{Al}_2\text{O}_3$	$\text{Fe}_2\text{O}_3$	$\text{Na}_2\text{O}$	$\text{K}_2\text{O}$	MnO	$\text{CaCO}_3$	$\text{MgCO}_3$
Minimum	0.00	0.00	0.00	0.00	0.001	0.000	0.00	91.11	0.02
Maximum	7.11	0.00	1.01	1.09	0.110	0.124	0.31	99.15	1.63

Table 3. The chemical composition of the two selected limestone samples from the Bełchatów deposit, Szczerców exploitation field (% by weight)

Tabela 3. Skład chemiczny dwóch wybranych próbek wapieni ze złoża węgla brunatnego Bełchatów, Pole eksploatacyjne Szczerców (% wag.)

Samples	SiO <sub>2</sub>	TiO <sub>2</sub>	Al <sub>2</sub> O <sub>3</sub>	Fe <sub>2</sub> O <sub>3</sub>	Na <sub>2</sub> O	K <sub>2</sub> O	MnO	CaCO <sub>3</sub>	MgCO <sub>3</sub>
Sample no. 1	2.51	0.02	0.04	0.11	0.003	0.003	0.02	97.15	0.06
Sample no. 2	1.08	0.00	0.13	0.06	0.008	0.004	0.00	98.51	0.02

Table 4. The reactivity (RI) [Ca/S moles] and absolute sorption index (CI) [gS/1000 g of the sorbent] of the two selected limestone samples from the Bełchatów deposit

Tabela 4. Wskaźniki reaktywności (RI) [Ca mol/S mol] i sorpcji bezwzględnej (CI) [g S/1000 g sorbentu] dwóch wybranych próbek wapieni ze złoża Bełchatów, Pole eksploatacyjne Szczerców

Samples	RI	CI	The assessment of sorption capacity
Sample no. 1	1.97	161.11	Excellent
Sample no. 2	3.10	102.16	Good

An X-ray analysis of the samples after the sulphurization process (Fig. 2) has shown that sample no. 2 is characterized by a low degree of conversion from SO<sub>2</sub>, which is confirmed by the CaO content at a level of approximately 18% by volume. In the case of phase composition of sample no. 1, only anhydrite has been determined.

In order to determine the parameters responsible for the highly variable sorption capacity of the analyzed samples, their phase composition was determined by the X-ray diffraction method. In addition to calcite, small amounts of quartz were identified. Then, the thermogravimetric analysis was performed. It was confirmed that both the decomposition temperature and the calcite decomposition rate, measured by weight loss, show no significant differences. The calcite decarbonization process starts at about 680°C and ends at about 879.2°C (sample no. 1) and 888.9°C. The calcite decomposition is accompanied by a weight loss which, at the temperature of 850°C, is 35.2% by volume (the sample no. 1) and 34.6% weight percent – sample no. 2. The degree of calcite decarbonization determined on this basis at the temperature of 850°C is 85.0% (sample 1) and 78.7% (sample 2), respectively.

Based on the analysis of porous texture parameters using low temperature nitrogen adsorption and mercury porosimetry, several key findings have been made (Table 5 and 6).

The specific surface area of the examined limestone samples determined using low temperature nitrogen adsorption is highly variable. Sample no. 2, with significantly less favorable, although relatively good sorption properties, has a significantly larger surface area than

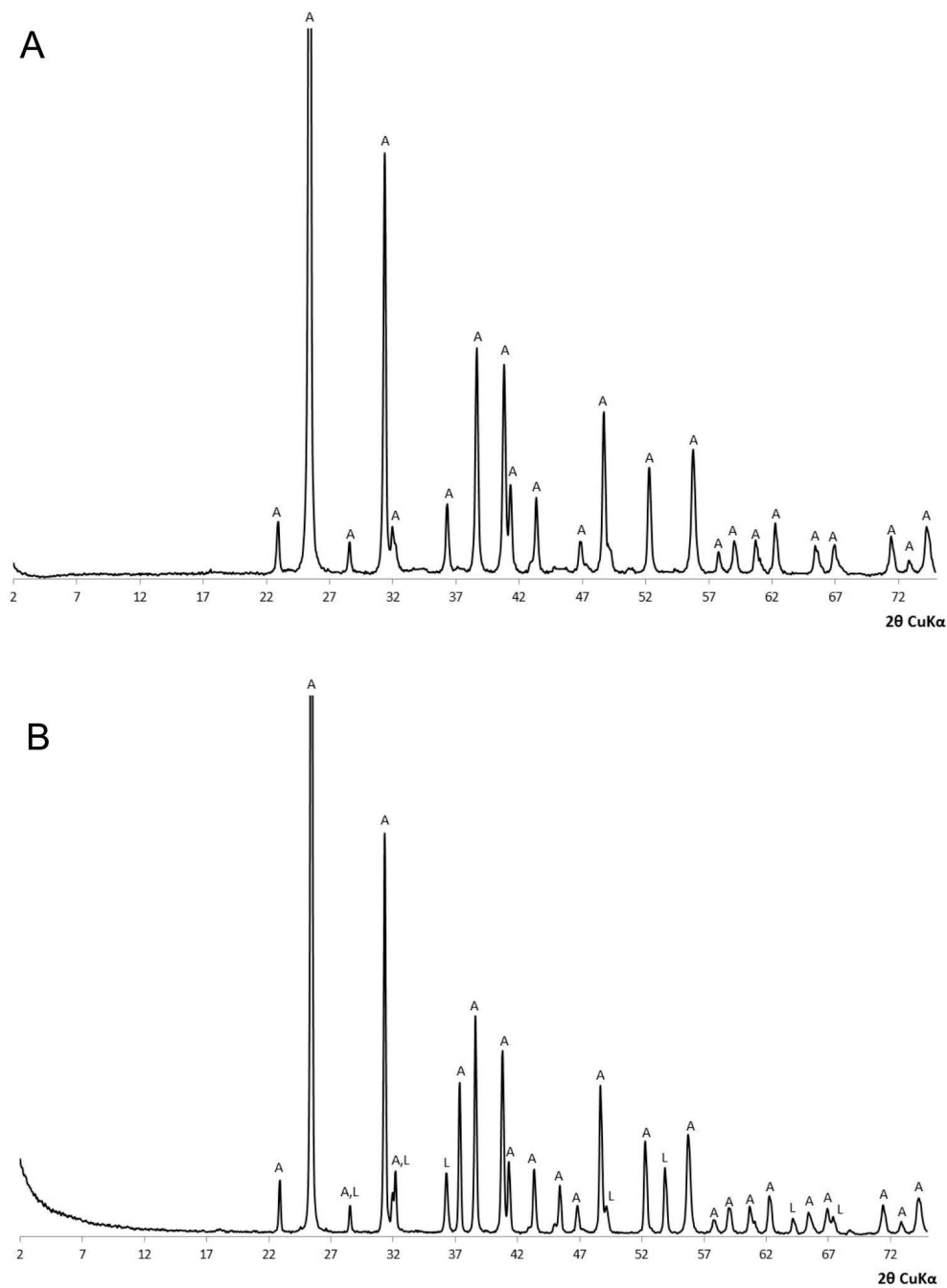


Fig. 2. Phase composition of the analyzed samples tested after the sulphurization process.  
 A – sample no. 1; B – sample no. 2. Explanations: A – anhydrite ( $\text{CaSO}_4$ ); L – Lime ( $\text{CaO}$ )

Rys. 2. Skład fazowy analizowanych próbek wapieni po procesie zasiarczania  
 A – próbka 1, B – próbka 2. Objaśnienia: A – anhydryt ( $\text{CaSO}_4$ ); L – wapno ( $\text{CaO}$ )



Table 5. The porous texture parameters determined by the low-temperature nitrogen sorption

Tabela 5. Parametry tekstury porowatej oznaczone z wykorzystaniem metody niskotemperaturowej sorpcji azotu

Parameter	Sample no. 1	Sample no. 2
$S_{\text{BET}}$ [m <sup>2</sup> /g]	1.8	12.2
$V_{\text{tot}}$ [cm <sup>3</sup> /g]	0.013	0.029
$V_{\text{mic}}$ [cm <sup>3</sup> /g]	0.000	0.004
$V_{\text{mic}}/V_{\text{tot}}$	0.000	0.138
$V_{\text{mes}}$ [cm <sup>3</sup> /g]	0.004	0.021
$V_{\text{mes}}/V_{\text{tot}}$	0.333	0.724
$V_{\text{mac}}$ [cm <sup>3</sup> /g]	0.008	0.004
$V_{\text{mac}}/V_{\text{tot}}$	0.667	0.138
$D_{\text{av}}$ [nm]	26.4	9.5
$D_{\text{av}}$ [μm]	0.0264	0.0095

Explanations:  $S_{\text{BET}}$  – the specific surface area,  $V_{\text{tot}}$  – the total pore volume;  $V_{\text{mic}}$  – the micropore volume,  $V_{\text{mic}}/V_{\text{tot}}$  the micropore share in the total pore volume;  $V_{\text{mes}}$  – the mesopore volume;  $V_{\text{mes}}/V_{\text{tot}}$  – the mesopore share in the total pore volume;  $V_{\text{mac}}$  – the macropore volume;  $V_{\text{mac}}/V_{\text{tot}}$  – the share of macropores in the total pore volume,  $D_{\text{av}}$  – the average pore diameter.

Table 6. The porous space parameters measured using mercury porosimetry for pore diameter range between 0.0005–1000 μm

Tabela 6. Parametry tekstury porowatej oznaczone z wykorzystaniem porozymetrii rtęciowej dla zakresu porów 0.0005–1000 μm

Sample	$S_{\text{POR}}$	$V_{\text{POR}}$	$P_{\text{POR}}$	$D_{\text{POR}}$
Sample no. 1				
Natural	0.99	0.36	46.53	1.49
After decarbonization	4.25	2.88	86.99	3.56
After SO <sub>2</sub> sorption	1.22	0.69	31.09	1.40
Sample no. 2				
Natural	1.43	0.39	28.72	0.82
After decarbonization	1.98	0.69	32.53	1.62
After SO <sub>2</sub> sorption	0.96	0.54	15.86	0.22

Explanations:  $S_{\text{POR}}$  – the specific surface area [m<sup>2</sup>/g];  $V_{\text{POR}}$  – the pore volume [mL/g];  $P_{\text{POR}}$  – the effective porosity [%];  $D_{\text{POR}}$  – the average pore diameter [μm].

the sample 1 with is characterized by excellent sorption properties. The large part of the surface area of sample no. 2 is determined on the basis of micropores and mesopores content (Table 5). In the case of sample no. 1, no micropores were found, while the amount of mesopores was clearly lower than for sample no. 2.

The analysis of porous texture parameters, determined using mercury porosimetry of natural samples and after the decarbonization and SO<sub>2</sub> sorption processes leads to interesting conclusions (Table 6). The examined samples in the natural state are characterized by the different size of the surface area (0.99 m<sup>2</sup>/g for sample 1 and 1.093 m<sup>2</sup>/g for sample 2). After the decarbonization process (thermal dissociation), the surface value of sample 1 significantly increases to a level of 4.25 m<sup>2</sup>/g, while in the case of sample 2 only a slight increase, up to 1.98 m<sup>2</sup>/g is recorded. After the SO<sub>2</sub> sorption process, the surface of the tested samples decreases to a level of 1.22 m<sup>2</sup>/g for sample 1 and 0.96 m<sup>2</sup>/g for sample 2. This is related to filling of the internal surface of the pores with calcium sulphate produced during the sulfation process.

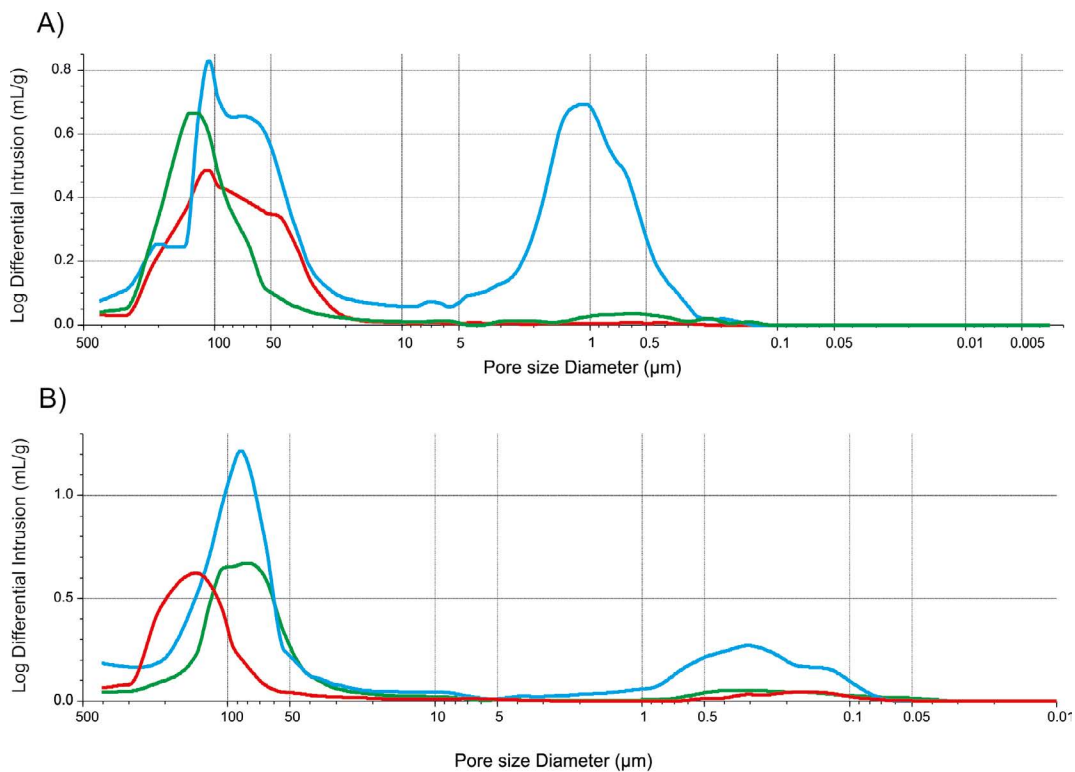


Fig. 3. The pore volume distribution as a function of their diameter, determined using mercury porosimetry.

Explanations: A – sample 1; B – sample 2;

— natural sample, — sample after the decarbonization, — sample after the SO<sub>2</sub> sorption

Rys. 3. Rozkład objętości porów w funkcji ich średnicy, wyznaczony z wykorzystaniem porozymetrii rtęciowej

Objaśnienia: A – próbka 1; B – próbka 2;

— próbka naturalna, — próbka po dekarbonatyzacji, — próbka po sorpcji SO<sub>2</sub>

The pore volume distributions as a function of their diameter presented in Fig. 3 show that the increase of the specific surface area growth during the decarbonization process occurs within pores with diameters of 0.3–2  $\mu\text{m}$  (sample 1, Fig. 3a) and 0.04–0.7  $\mu\text{m}$  (sample 2, Fig. 3b). The pore volume in dissociated samples is highly variable: sample 1 – 2.88 mL/g; sample 2 – 0.69 mL/g (Table 6). After the sulphation process, the pores in the mentioned diameter range disappear completely only in the case of sample 1. In the case of sample no. 2, some of them are still present. The analysis of another porous texture parameter, effective porosity, is also interesting. For sample no. 1, the value of this parameter is higher in each case (Table 6), which indicates the free flow of gases through the grains of the sample no. 1.

The abovementioned porous texture characteristics are well illustrated by the micro images presented below made using a scanning electron microscope (Electron Backscatter Diffraction) and showing the morphology of the limestone surface in the natural state after the decarbonization and  $\text{SO}_2$  sorption processes (Figs. 4–10).

The analysis of the surface morphology, presented in the above micro images, indicates a high variability, that is a clear distinction between the structural and textural characteristics of the examined samples. In its natural state sample no. 1 is characterized by a micro-sparitic structure and porous texture. Particular attention is paid to the pores and slots between the sparitic calcite crystals (Fig. 4). Sample no. 2 is made of micric calcite crystals. The porous texture of this sample is poorly marked. The pores are small in size and are barely visible (Fig. 5).

Images 6 and 7 confirm that the release of  $\text{CO}_2$  from the calcite structure leads to the development of porosity and the related increase of the specific surface area. There is a clear

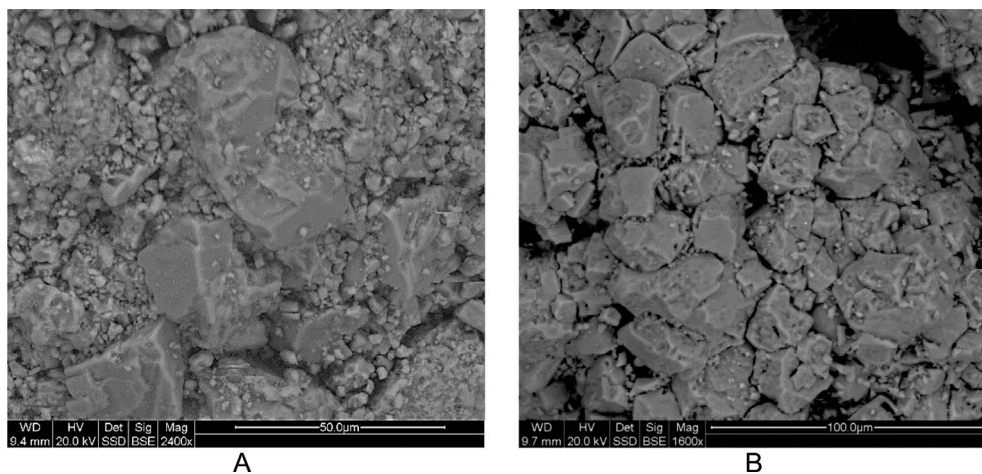


Fig. 4. Sample no. 1 – natural state. The visible micro-sparitic (A) and sparitic sorbent structure with clearly marked porous texture (B)

Rys. 4. Próbkę 1 – stan naturalny. Widoczna mikrytowo-sparytowa (A) i sparytowa struktura sorbentu z wyraźnie zaznaczoną porowatą teksturą (B)

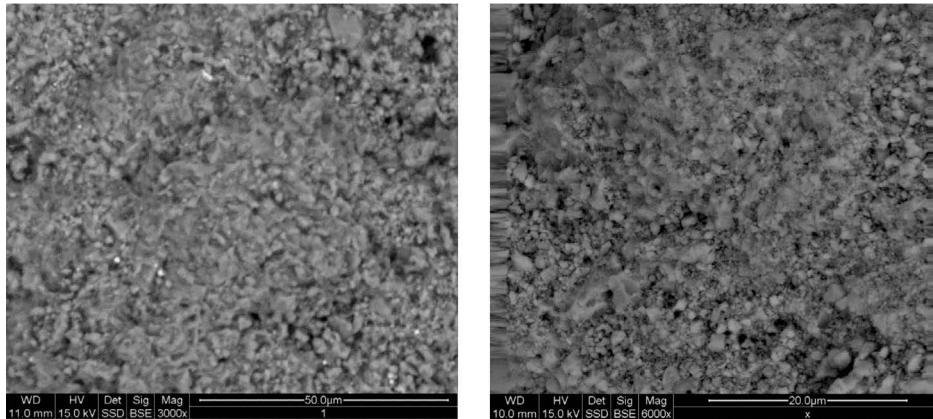


Fig. 5. Sample no. 2 – natural state. The visible micrite structure with very poorly marked porous texture

Rys. 5. Próbką 2 – stan naturalny. Widoczna mikrytowa struktura z bardzo słabo zaznaczoną teksturą porowatą

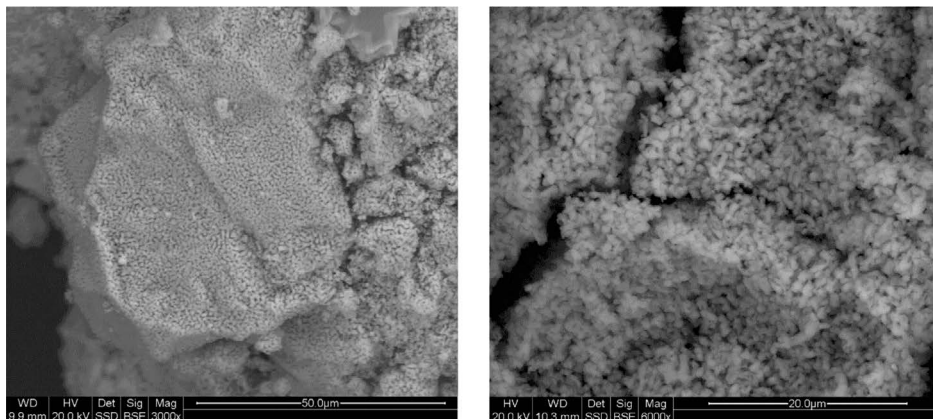


Fig. 6. The SEM image of grain surface of the sample no. 1 after the decarbonization process

Rys. 6. Próbką 1 – powierzchnia ziaren po procesie dekarbonatyzacji

difference in the development of surface areas between the samples. These differences are determined by the pore size. The pores formed in sample no. 1 have significantly larger diameters (Fig. 6) than those in sample no. 2 (Fig. 7). This variation in pore size plays a key role when determining the specific surface area using mercury porosimetry. This is due to the fact that the mentioned method is used to measure pores with diameters greater than 5 nm, which means that the micropores and part of the mesopores are ignored during the measurement process. In the case of sample no. 2, the lower value of the specific surface area after the decarbonization process (Table 6) is related to the formation of pores with diameters less than 5 nm. Clear differences between the structural characteristics are also visible

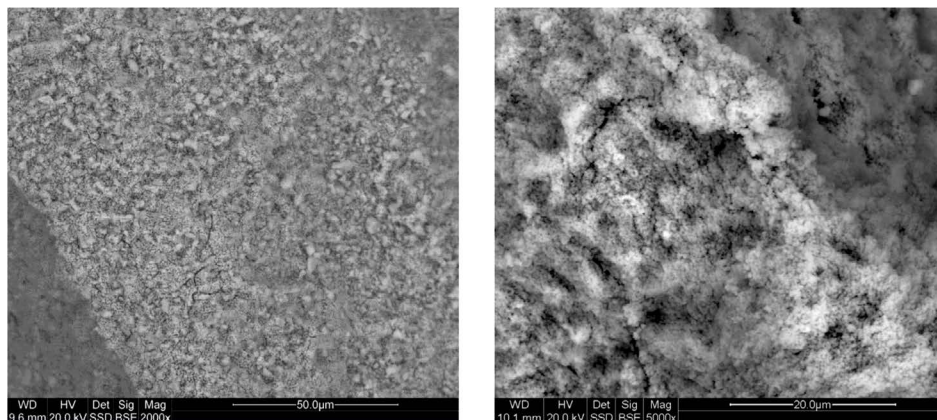


Fig. 7. The SEM image of grain surface of the sample no. 2 after the decarbonization process

Rys. 7. Próbką 2 – powierzchnia ziaren po procesie dekarbonatyzacji

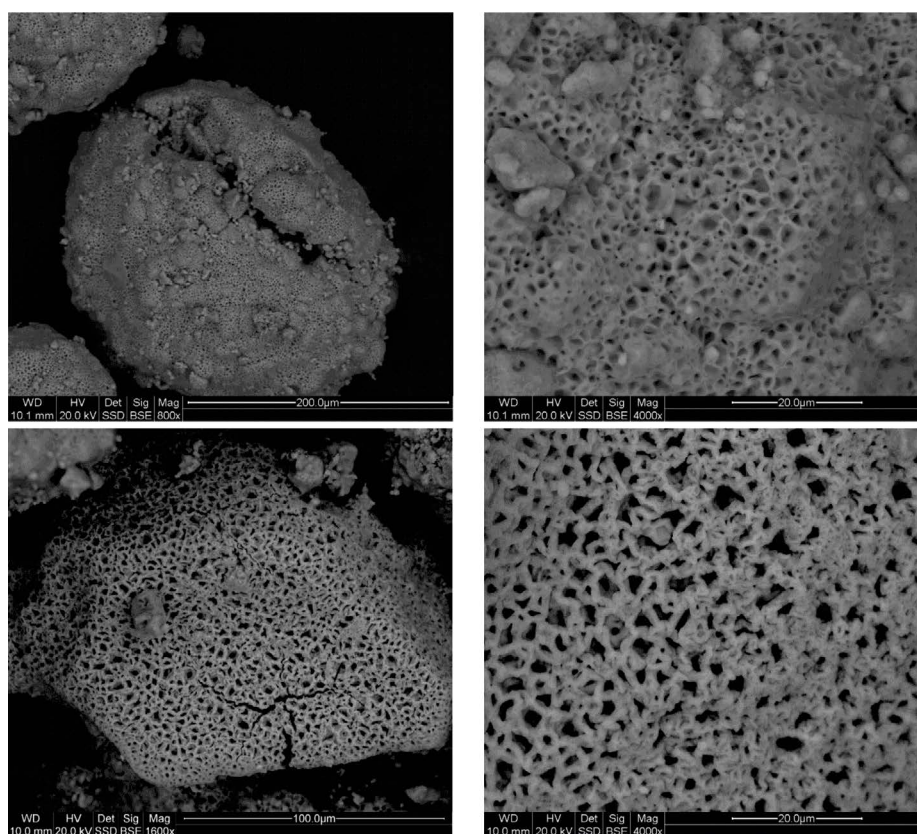


Fig. 8. The SEM image of grains surface of the sample no. 1 after the sulphurization process.  
Grains coated with calcium sulphate with a porous texture

Rys. 8. Próbką 1 – powierzchnia ziaren po procesie zasiarczania.  
Ziarna pokryte siarczanem wapnia o teksturze porowatej

in the sulphated samples. In the case of sample no. 1, the sorbent grains were coated with calcium sulphate with a porous texture (Fig. 8). The pores are open and the diameters reach up to several micrometers. In turn, massive sulphate incrustation, almost completely free of open pores, was formed on the grain surface of sample no. 2 (Fig. 9).

The variable efficiency of  $\text{SO}_2$  sorption between the examined samples is well illustrated by the SEM micro-images presented below showing the cross-sections of sulphur grains and the sulphur content analysis (Energy-Dispersive X-ray Analysis, EDX) carried out in

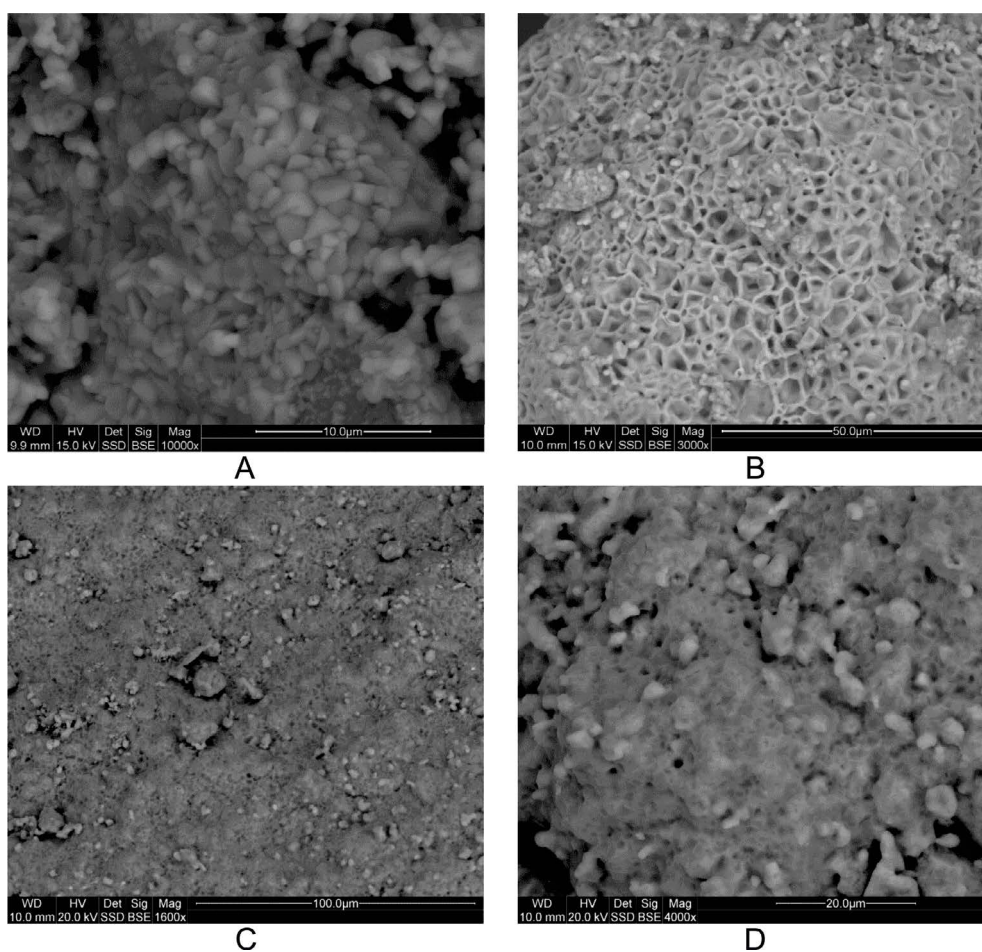


Fig. 9. The SEM image of grain surface of the sample no. 2 after the sulphurization process. The surface of the sorbent grain is coated with calcium sulphate: of crystalline formation with no visible signs of porosity (A); of pseudo-crystalline formation and massive texture with visible surface pores (B); and of pseudo-crystalline formation with a few open pores (C, D)

Rys. 9. Próbką 2 – powierzchnia ziaren po procesie zasiarczania. Powierzchnia ziarna sorbentu pokryta siarczanem wapnia: o krystalicznym wykształceniu bez widocznych oznak porowatości (A); krypto krystalicznym wykształceniu i teksturze masywnej, widoczne pory powierzchniowe (B); kryptokrystalicznym wykształceniu z nielicznymi porami otwartymi (C, D).

the points marked on the images (Fig. 10 and 11; Table 7). There are clear differences in the degree of reaction between the CaO and SO<sub>2</sub> within the individual grains of the samples. In the case of sample no. 1, both the outer and inner surface of the grain reacted in a similar way (Fig. 10). Meanwhile, there are two distinct reaction zones within the grains of the sample no. 2: the outer one with a significant sulphur content and thus a high degree of reactivity and the inner one with a significantly lower sulphur content, indicating a low degree of CaO use (Fig. 11).

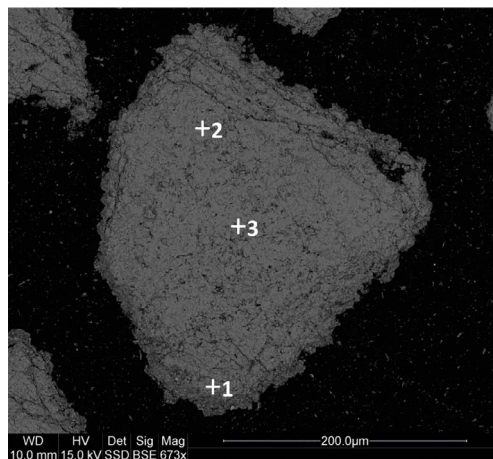


Fig. 10. The SEM image of the cross section of the grain (sample no. 1) after the sulphurization process  
1, 2, 3 – EDX points

Rys. 10. Próbką 1 – ziarno po procesie zasiarczania w przekroju poprzecznym.  
1, 2, 3 – punkty, w których wykonano analizę EDX

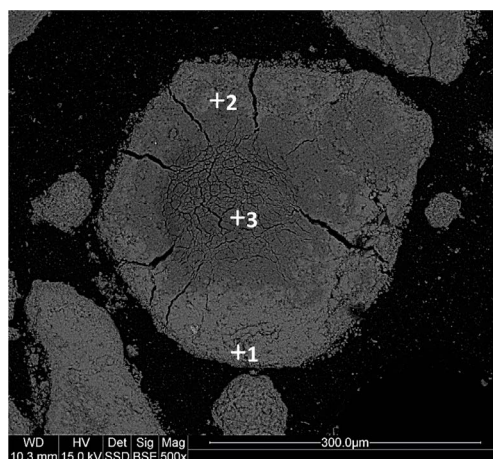


Fig. 11. The SEM image of the cross section of the grain (sample no. 2). 1, 2, 3 – EDX points

Rys. 11. Próbką 2 – ziarno po procesie zasiarczania w przekroju poprzecznym.  
1, 2, 3 – punkty, w których wykonano analizę EDX

Table 7. Sulphur content in the sample collection points marked on the pictures (Figures 11 and 12)

Tabela 7. Zawartość siarki w zaznaczonych na fotografii punktach pomiarowych (rys. 11 i 12)

Sample collection point	Sulphur content [% by weight.]
Sample no. 1	
1.	21.9
2.	21.2
3.	19.8
Sample no. 2	
1.	20.5
2.	5.1
3.	–

### 3. Discussion

The results of the study confirm the conclusions of numerous researchers that the main limitation of dry desulphurization methods, also in the case of fluidized bed combustion, is the low utilization rate of the sorbent (rarely exceeding 30–40%) (Dam-Johansen and Østergaard 1991; Yao et al. 2010), manifested by the presence of unreacted or even non-dissolved sorbent residues in interiors/centers of grains. They indicate that the structural and textural nature of the sorbent, developed during the decarbonization process as a result of the release of CO<sub>2</sub> from the calcite, has a decisive impact on the SO<sub>2</sub> absorption efficiency during the dry flue gas desulphurization process. The SO<sub>2</sub> adsorption takes place on the internal surface of pores formed during the decarbonization process (Yao et al. 2010). The reactivity of the sorbent is determined by the size of the surface area capable of reacting with SO<sub>2</sub>. A surface capable of reacting with SO<sub>2</sub> should be based on a system of interconnected pores with sufficiently large diameters. This is indicated by the values of porous texture parameters determined using the mercury porosimetry, including, among others, the porosity efficiency (32.53% for sample no. 1; 86.99% for sample no. 2) and the average pore diameter (1.62 μm for sample no. 1; 3.56 for sample no. 2) (Table 6). An analysis of the pore volume distributions, presented as a function of the diameter of natural samples after the decarbonization and SO<sub>2</sub> sorption processes (Fig. 3), suggests that pores with a diameter above 0.06 μm (i.e. meso and macropores) take part in the SO<sub>2</sub> sorption process. If the surface is made of pores with smaller diameters (from the assumed 0.06 μm) then it will be inaccessible for SO<sub>2</sub>. The sorption process will occur only on the outer surface of the sorbent grains (Fig. 11). The outer grain surface will be coated by the resulting desulphurization product and the interior of the grain will become inaccessible to the SO<sub>2</sub> particles and will remain unused.



Under real conditions (where decarbonization and SO<sub>2</sub> sorption processes take place simultaneously), the structural and textural characteristics of a limestone/sorbent will be of great importance for the SO<sub>2</sub> sorption process, both before the thermal dissociation and after the calcium sulphate (desulphurization product) is produced on the grain surface of the sorbent as a result of reaction with SO<sub>2</sub>. Also in this case, the porosity system described above will play a very important role. The difference is the occurrence of pores with a diameter in the range of micrometers and all types of textural, tectonic, and compaction discontinuities (such as stylolite seams) (Hycnar 2015) and slots between calcite crystals presented in Fig. 4b. Such porous texture elements play a role of channels of CO<sub>2</sub> and SO<sub>2</sub> diffusion from and into the interior (center) of sorbent grains, respectively; therefore, they are intensifying the decarbonization and SO<sub>2</sub> sorption processes. The porous texture of calcium sulphate produced on the grain surface is also of key importance. The porosity guarantees the free flow of SO<sub>2</sub>, resulting in a uniform sulphation of grains during the sorbent residence time in the installation (Pacciani et al. 2009). If a pore-free sulphate is formed on the surface of sorbent grains (Fig. 9), the SO<sub>2</sub> sorption will be stopped at the initial stage of desulphurization process, resulting in low use of the sorbent manifested by the occurrence of unreacted (also non-dissociated in the case of industrial conditions) interiors/centers of grains (Anthony and Granatstein 2001).

The presented results allow for concluding that in the case of dry desulphurization methods, the high content of CaCO<sub>3</sub> in the sorbent does not guarantee the high efficiency of the desulphurization process. The efficiency of the SO<sub>2</sub> capture is largely dependent on the structural and textural characteristics of limestone (sorbent), particularly on the porosity of the sorbent (Laursen et al. 2000). Limestones with a well-developed porosity system based on larger mesopores and macropores are predisposed to produce sorbents dedicated to fluidized bed combustion technology. In turn, the porous textures formed by micropores and smaller mesopores will adversely affect the sorption properties of limestone.

## Summary

The structural and textural characteristics, including porosity, are an individual feature of limestones, formed as a result of sedimentation, diagenesis, and epigenesis. The structural and textural characteristics of the examined limestones, described in detail by Hycnar (2015), are the result of the calcite dissolution and recrystallization processes occurring under varying environmental conditions. In order to predict the limestone/sorbent behavior under industrial conditions already at the laboratory stage, there is a need to improve the quality research methodology with the addition of porous texture analysis (Yrjas et al. 1995). A key element of the analysis will be the designation of the area capable of reacting with SO<sub>2</sub> under conditions of actual fluidized bed boilers. As shown in the discussion, this type of research should be conducted with the use of limestone samples in the natural state, after the decarbonization and SO<sub>2</sub> sorption processes, while the proper selection of the test method

is of great importance. The porous texture parameters, including the specific surface area, pore volume, pore diameter, and the effective porosity, determined using mercury porosimetry, provided important information on the SO<sub>2</sub> sorption mechanism under fluidized bed conditions

The measurement of limestone quality (and other carbonate rocks, e.g. dolomites) for the needs of dry desulphurization methods should be accompanied by, in addition to chemical composition, the RI reactivity index, and absolute sorption index (CI) analyses, the porous texture analysis using mercury porosimetry. The presented research methods, that were selected already at the laboratory stage, will allow to predict the limestone/sorbent behavior under industrial conditions.

*The work is statutory activities of the Department of Mineralogy, Petrography and Geochemistry of the AGH University of Science and Technology in Cracow in 2018.*

## REFERENCES

- Alsthrom Propywe-Reactivity index. Alsthrom Propywer 1995.
- Anthony, E.J. and Granatstein, D.L. 2001. Sulfation phenomena in fluidized bed combustion systems. *Progress in Energy and Combustion Science* 27, pp. 215–236.
- AutoPore IV 9520 Operator's Manual V1.09, 2008, Micromeritics Instrument Corporation, 950-42801-01.
- Borgwardt, R.H. 1985. Calcinations Kinetics and Surface Area of Dispersed Limestone Particles. *AIChE Journal* 31, pp. 355–362.
- Dam-Johansen, K. and Østergaard, K. 1991. High-temperature reaction between sulphur dioxide – 1. Comparison of limestones in two laboratory reactors and a pilot plant. *Chemical Engineering Science* 46, 3, pp. 827–37.
- Galos et al. 2016 – Galos, K., Szlugaj, J. and Burkowicz, A. 2016. Sources of limestone sorbents for flue gas desulphurization in Poland in the context of the needs of domestic power industry. *Polityka Energetyczna – Energy Policy Journal* 19, 2, pp. 149–170 (in Polish).
- Hycnar, E. 2015. Structural-textural nature and sorption properties of limestones from the mesozoic-neogene contact zone in the Belchatów deposit. *Gospodarka Surowcami Mineralnymi – Mineral Resources Management* 31, 4, pp. 75–94.
- Hycnar et al. 2012 – Hycnar, E., Ratajczak, T. and Nieć, M. 2012. The “Zalas” porphyry deposit – problem of accompanying minerals still current?. *Opencast Mining* 53, 1–2, pp. 9–14 (in Polish).
- Hycnar et al. 2015 – Hycnar, E., Ratajczak, T. and Jończyk, M.W. 2015. Carbonate associated minerals and possibilities for their utilization as SO<sub>2</sub> sorbents (on the example „Belchatów” lignite deposit). *Bulletin of the Mineral and Energy Economy Research Institute of the Polish Academy of Sciences* 90, pp. 19–31 (in Polish).
- Hycnar et al. 2016 – Hycnar, E., Ratajczak, T., Jonezyk M.W. and Wal M. 2016. The possibilities of using chalk from domestic deposits in flue gas desulphurization technologies used in the energy sector. *Zeszyty Naukowe Instytutu Gospodarki Surowcami Mineralnymi i Energią PAN* 96, pp. 71–80 (in Polish).
- Laursen et al. 2000 – Laursen, K., Duo, W., Grace, J.R. and Lim, J. 2000. Sulfation and reactivation characteristics of nine limestones. *Fuel* 79, pp. 153–63.
- Mohammad et al. 1988 – Mohammad, R., Hajaligol, J.P., Longwell, A.F. and Sarofim, H. 1988. Analysis and modeling of the direct sulfation of CaCO<sub>3</sub>. *Ind. Eng. Chem. Res.* 27, 12, pp. 1543–1549.
- Pacciani et al. 2009 – Pacciani, R., Müller, C.R., Davidson, J.F., Dennis, J.S. and Hayhurst, A.N. 2009. The Performance of a Novel Synthetic Ca-Based Solid Sorbent Suitable for the Removal of CO<sub>2</sub> and SO<sub>2</sub> from Flue Gases in a Fluidised Bed. *Proceedings of the 20th International Conference on Fluidized Bed Combustion, Environmental and Pollution Control*, pp. 972–978.

- Rootare, H.M. and Prezlow, C.F. 1967. Surface Areas from Mercury Porosimetry Measurements, *J. Phys. Chem.*, pp. 2733–2736.
- Such, P. 2000 – The pore space investigations for geological and engineering purposes. *Scientific Works of the Oil and Gas Institute* 104, 96 pp.
- Such P. 2002 – An application of mercury porosimetry in pore space investigations. *Scientific Works of the Oil and Gas Institute* 113, 86 pp.
- Szymanek, A. and Nowak W. 2007. Mechanically activated limestone. *Chemical and Process Engineering* 287, pp. 127–137.
- Yao et al. 2010 – Yao, X., Zhang, H., Yang, H., Liu, Q., Wang, J. and Yue, G. 2010. An experimental study on the primary fragmentation and attrition of limestones in a fluidized bed. *Fuel Processing Technology*.
- Yrjas et al. 1995 – Yrjas, P., Iisa, K. and Hupa, M. 1995. Comparison of SO<sub>2</sub> capture capacities of limestones and dolomites under pressure. *Fuel* 74, 3, pp. 395–400.

#### CHARAKTER STRUKTURALNO-TEKSTURALNY WAPIENI A EFEKTYWNOŚĆ SORPCJI SO<sub>2</sub> W WARUNKACH PALENISK FLUIDALNYCH

##### Słowa kluczowe

porowatość, sorbenty SO<sub>2</sub>, wapienie, siarczanowanie

##### Streszczenie

Przedstawiono rezultaty badań właściwości sorpcyjnych wapieni względem SO<sub>2</sub> w warunkach palenisk fluidalnych. Udowodniono, że decydujący wpływ na efektywność wychwytu SO<sub>2</sub> ma charakter strukturalno-teksturalny sorbentu, który kształtuje przebieg procesu siarczanowania, a nie jak się powszechnie przyjmuje się – zawartość CaCO<sub>3</sub> w sorbencie. Pokazano jak porowatość sorbentu wpływa na przebieg procesu sorpcji SO<sub>2</sub>. Określono parametry sorbentu, które powinny podlegać ocenie na etapie kwalifikowania surowca do produkcji sorbentów. Zaprezentowano metody badawcze, za pomocą których na etapie badań laboratoryjnych można w sposób precyzyjny przewidzieć reaktywność sorbentu w warunkach przemysłowych. Prezentowane w niniejszym artykule badania nad reaktywnością wapieni względem SO<sub>2</sub> zainspirowane zostały problemami polskich elektrowni i elektrociepłowni związanymi z dotrzymaniem limitów emisji SO<sub>2</sub> podczas stosowania wapieni jako sorbentów SO<sub>2</sub> w paleniskach fluidalnych, niskim stopniem wykorzystania sorbentów, wysoką zawartością nieprzereagowanego CaO w popiołach i problemami związanymi tak z ich wykorzystaniem jak i składowaniem. Badania prowadzono przez kilka lat. W tym czasie przebadano kilkaset próbek wapieni wieku kredowego (kreda piszcząca), jurajskiego, triasowego, dewońskiego i neogeńskiego (kreda jeziorna). Rezultaty badań są w stanie przyczynić się do zwiększenia stopnia wykorzystania, sorbentu i co za tym idzie podniesienia efektywności wychwytu SO<sub>2</sub> w warunkach palenisk, a przez to znacząco ograniczyć ilość powstających odpadów paleniskowych.

**THE STRUCTURAL AND TEXTURAL CHARACTERISTICS OF LIMESTONES  
AND THE EFFECTIVENESS OF SO<sub>2</sub> SORPTION IN FLUIDIZED BED CONDITIONS**

**Key words**

porosity, limestone, SO<sub>2</sub> sorbents, sulphation process

**Abstract**

The results of studies on the sorption properties of limestone with respect to SO<sub>2</sub> under fluidized bed conditions are presented. It has been confirmed that the structural and textural characteristics of limestones (which, contrary to the common belief, are shaping the course of the sulphation process rather than the CaCO<sub>3</sub> content) have a decisive influence on the effectiveness of SO<sub>2</sub> capture. The impact of the porosity of limestones on the SO<sub>2</sub> sorption process has been shown. Limestone parameters, which should be assessed at the stage of qualification of raw material for raw material production, have also been determined. The research methods, which can be used to predict the reactivity of sorbent in industrial conditions at the stage of laboratory analysis, have been presented. Presented in this article studies on the reactivity of limestone terms of SO<sub>2</sub> were inspired by the problems of Polish power plants in meeting the SO<sub>2</sub> emission limits when using limestones as SO<sub>2</sub> sorbents in fluidized bed boilers and related to their low utilization and storage, and the high content of unreacted CaO in the ash. The studies have been conducted for several years. In that time, been tested several hundred samples limestone of Cretaceous (chalk), Jurassic, Triassic, Devonian, and Neogene (lacustrine chalk) age. The results of the study can contribute to the increased use of sorbent and thus increase the efficiency of SO<sub>2</sub> capture in furnace conditions and, as a consequence, significantly reduce the amount of the combustion waste generated.